Published in final edited form as:

Ultrasound Obstet Gynecol. 2022 March ; 59(3): 358–364. doi:10.1002/uog.23753.

B-flow/Spatio-Temporal Image Correlation M-Mode: A Novel Ultrasound Method that Detects a Decrease in Spiral Artery Luminal Diameter in the First Trimester in a Primate Model of Impaired Spiral Artery Remodeling

O.M. Turan[1], **J.S. Babischkin**[1], **G.W. Aberdeen**[1], **S. Turan**[1], **C.R. Harman**[1], **G.J. Pepe**[2], **E.D. Albrecht**[1]

[1]Department of Obstetrics, Gynecology, and Reproductive Sciences, University of Maryland School of Medicine, Baltimore, MD

[2]Department of Physiological Sciences, Eastern Virginia Medical School, Norfolk, VA

Abstract

Objective: To determine if B-flow/spatio-temporal image correlation (STIC) M-mode ultrasonography detects a decrease in spiral artery luminal diameter and volume flow during the first trimester in a nonhuman primate model of impaired spiral artery remodeling (SAR).

Methods: Baboons were treated with estradiol on days 25–59 of the first trimester of pregnancy (term = 184 days). Spiral artery luminal diameter and volume flow were quantified by B-flow/STIC M-mode ultrasonography on day 60 of gestation and results compared with the percentage of spiral arteries remodeled by extravillous trophoblasts as quantified *ex vivo* by immunohistochemical image analysis on placental basal plate tissue collected via cesarean section on day 60.

Results: The percentage of spiral arteries greater than 50 μm in diameter remodeled by extravillous trophoblasts was 70% lower (P = 0.000001) in estradiol-treated baboons than in untreated animals. Spiral artery luminal diameter at systole and diastole, as quantified by B-flow/STIC M-mode in the first trimester of pregnancy, was 32% (P = 0.014) and 50% (P = 0.005) lower, respectively, and volume flow 85% lower (P = 0.014) in SAR suppressed baboons than in untreated animals. There was a significant (P < 0.05) correlation between the level of spiral artery luminal diameter as quantified by B-flow/STIC M-mode ultrasonography and level of SAR.

Conclusion: B-flow/STIC M-mode ultrasonography provides a novel real-time noninvasive method to detect a decrease in uterine spiral artery luminal diameter and volume flow during the cardiac cycle in the first trimester in a nonhuman primate model of defective SAR.

Keywords

B-flow; STIC; M-mode; ultrasound; primate; uterine; spiral artery diameter; remodeling

Address correspondence to Eugene D. Albrecht, Ph.D., Department of Obstetrics, Gynecology and Reproductive Sciences, University of Maryland School of Medicine, Baltimore, MD 21201, ealbrecht@som.umaryland.edu.

INTRODUCTION

During the first trimester of pregnancy, the uterine spiral arteries are remodeled (SAR) by extravillous trophoblasts into high-capacity vessels with enlarged lumens to promote placental perfusion. A defect in SAR underlies early onset preeclampsia, fetal growth restriction and pre-term birth[1–3]. Non-invasive real-time imaging methods to assess spiral artery dynamics that reflect impaired SAR early in gestation would be invaluable to diagnose abnormal human pregnancy caused by defective SAR. However, an *in vivo* assessment tool to reliably quantify impaired SAR has not been developed. Although uterine artery flow resistance is currently used as a proxy marker for impaired placentation, its value in the first and second trimesters as a stand-alone test is limited.[4–6] Histological studies clearly show that extensively remodeled spiral arteries have a thin wall that accommodates increased blood flow, whereas poorly remodeled vessels retain a thickened wall and narrow lumen[7]. However, histological detection of impaired UAR has been made on tissue obtained after birth[1,2] and thus not of timely use to predict at risk pregnancy. Since the main change in SAR is in the blood vessel architecture, an imaging method that could quantify in real time vessel dimension reflecting wall movements against flow during the cardiac cycle would be the best test to identify differences in proper and improper SAR. In addition, the method should be validated with immunohistochemical assessment of the level of SAR at the time of imaging.

We have established, by slightly elevating estradiol levels early in baboon pregnancy, a highly specific, selective and reproducible model of defective SAR[8,9]. Pregnant baboons exhibit uterine vascular anatomy, the maternal-placental-fetal endocrine axis and SAR similar to human pregnancy[10]. The defect in SAR was associated late in gestation with reduced uterine artery flow, increased maternal serum sFlt-1 levels, hypertension, and maternal vascular dysfunction, which are hallmarks of human preeclampsia[8,9,11–13] (Table 1). We propose that this primate paradigm provides an innovative model to establish new real-time imaging approaches to assess aspects of SAR.

Ultrasound B-flow is a non-Doppler technology to assess vessels of the fetal heart and other organs[14–16]. B-flow provides high-contrast resolution for sharp rendering of vessel structure, however, it does not allow for functional measurements. Spatio-Temporal Image Correlation (STIC) reconstructs a volumetric data set from over 1500 image slices in 5 transverse planes and synchronizes volumetric data with the pulse. M-mode ultrasound generates spatial formation along the sound beam axis with high temporal resolution to digitally quantify vessel dimension/diameter. We hypothesize that spiral artery wall luminal diameter, resulting from movement during systole and diastole, is lower in poorly remodeled spiral arteries. To test this hypothesis we combined B-flow/STIC with M-Mode to quantify spiral artery luminal diameter during systole and diastole and compared imaging results with *ex vivo* immunohistochemical quantification of SAR during the first trimester of baboon pregnancy.

METHODS

Animals:

The present study was conducted in accordance with the ARRIVE (Animal Research: Reporting of *In Vivo* Experiments) guidelines to enable evaluation of the rigor and reproducibility of the methods, statistical analysis and results. Baboons *(Papio anubis)* were obtained from the Southwest National Primate Research Center (San Antonio, TX), housed individually in large primate cages, and received standard primate chow (Teklad Primate Diet 2050; Envigo, Frederick, MD) and fresh fruit twice daily and water *ad libitum*. Females were paired with male baboons for 5 days at the anticipated time of ovulation as estimated by menstrual cycle history and the pattern of external sex skin turgescence. Day 1 of pregnancy was designated as the day preceding perineal deturgescence. Baboons were cared for and used strictly in accordance with the United States Department of Agriculture regulations and the National Institutes of Health *Guide for the Care and Use of Laboratory Animals* (8^{th} ed.). The present experimental protocol was approved by the Institutional Animal Care and Use Committee of the University of Maryland School of Medicine.

Pregnant baboons were untreated or treated daily on days 25 to 59 of gestation with estradiol benzoate (25 μg/kg body weight/day sc in 1.0 ml of sesame oil). On day 60 of gestation (i.e. near end of first trimester; term = 184 days), baboons were lightly anesthetized with propofol/ketamine administered intravenously and supplemented with oxygen (1 L/min) to maintain SpO_2 > 95% and blood pressure and heart rate constant. B-flow/STIC M-mode ultrasound imaging of the uterine spiral arteries was performed as described below on day 60 in 7 untreated and 12 estradiol-treated baboons. Fifteen untreated and 18 estradiol-treated baboons were anesthetized with isoflurane, and subsequently, blood samples (2 ml) obtained from the maternal saphenous vein and the placenta removed by cesarean section for immunohistochemical quantification of SAR. B-flow/STIC M-mode ultrasound and quantification of SAR was simultaneously performed on 9 of these baboons, because either baboons were carried to term as part of another study or ultrasound imaging was unable to be performed. Serum estradiol levels were determined by RIA using an automated chemiluminescent immunoassay system (Immulite; Diagnostic Products Corp., Los Angeles, CA, USA) to confirm estradiol treatment. Intra-assay and inter-assay coefficients of variation were 6.9% and 7.3%, respectively.

Ultrasound B-flow/STIC M-mode quantification of spiral artery luminal diameter and volume flow:

Ultrasound B-flow/STIC M-mode imaging was performed on 7 untreated and 12 estradiol-treated baboons using a GoldSeal Voluson E8 (GE Health) and a 3D/4D transducer (RAB6-D ultralight 4–8.5 MHz STIC Convex). Fig. 1 illustrates the B-flow/STIC M-mode technique. Spiral arteries in the decidua basalis were identified in an untreated baboon using power and pulse Doppler (panel A). Spiral artery location was systemically selected at 2–4 cm interval sectors starting from the cord insertion of the placenta (defined as origin). Following B-flow activation the same spiral artery shown in panel A was located (panel B). Volume data sets representing multiplanar sequences of the vessels were then acquired in 4D STIC mode (10 sec, 25 degree angle). Archived 4D block images were obtained from

6 randomly selected regions, using a computer-generated number sequence[17]-to minimize bias, for offline quantification of vessel diameters. Post-processing analyses were performed utilizing 4D viewer and the multiplanar modality, which allows for simultaneous display of images in three orthogonal planes (which correspond to X, Y and Z axes, panel C). Image magnification was adjusted to 1.8 and upon identification of the same vessel in each dimensional plane, the M-mode was activated with a sweep speed of 2. M-mode gate was positioned on the vessel perpendicular (90 degrees) to the vessel lumen and vessel luminal diameter, reflecting wall movement during systole and diastole, determined (panel D). Arterial luminal diameter reaches a maximum in mid systole, which is immediately after peak arterial pressure, and vessel luminal diameter decreases towards end diastole as pressure declines. The luminal diameters of the vessel at the largest (systole) and smallest (diastole) segments were measured using a caliper and expressed in mm. Using the M-mode time measurement function, the duration of systole and diastole were measured and expressed as milliseconds. Each spiral artery was measured three times and the mean assigned as diameter of the blood vessel lumen during elapsed time for systole and diastole. The mean (± SE) coefficient of variation for repeated B-flow/STIC M-mode measurement of luminal diameter of each vessel at systole was 7.9 ± 1.1%. The minimum detectable luminal diameter of a spiral artery as assessed by B-flow/STIC M-mode in early baboon pregnancy approximated 0.1 mm. Panels E and F of Fig. 1 show B-flow/STIC and M-mode measurement of vessel luminal diameter at diastole (1) and systole (2) in a remodeled distensible spiral artery of an untreated baboon (panel E) and a non-remodeled spiral artery in a SAR suppressed baboon (panel F). The luminal diameter of the vessel in the SAR impaired baboon (Fig. 1F) appeared lower at systole (0.6 mm) and diastole (0.5 mm) than of the vessel in the untreated animal (1.8 mm and 1.0 mm, respectively, Fig. 1E).

Volume flow was calculated using the following formula: $\pi \times (D/2)^2 \times ((S \times T_S) + (D \times T_D))/(T_S+T_D)$. S: Systolic diameter, D: Diastolic diameter, T_S: Time for systole, T_D: Time for diastole. All B-flow/STIC M-mode measurements were performed by a single investigator (OMT).

The following criteria ensured B-flow/STIC M-mode authentication, optimization, standardization and quality control: (a) the spiral artery was visible in all 3 dimensions within the field of the acquired block; (b) the gate of the M-mode was positioned at 90 degrees to the vessel lumen; (c) quantification of the luminal diameter at systole and diastole determined by pulse Doppler measurement of heart rate was compared with maternal pulse; (d) independence of the transmit angle and almost artifact-free depiction of artery structure to assure accurate high-resolution assessment of vessel dimension; (e) correlation of visua1 pulsatility identified in the artery was depicted with the documented arterial pulse; and (f) arteries were differentiated from veins by their flow properties. Moreover, spiral artery luminal diameter and volume flow, as determined by B-flow/STIC M-mode, did not show a change in the values obtained at the area of cord insertion and near the margins of the placenta.

In an ongoing companion study of B-flow/STIC M-mode in human subjects, obtaining the 4D block images adds 5–8 minutes to the routine ultrasound examination in the first, second and third trimesters, while offline post-processing analysis takes 20–30 minutes per subject.

If the offline measurements are completed at the time of obtaining the 4D block, the total exam would be prolonged by only 15–20 minutes. B-flow/STIC M-mode imaging of the spiral arteries in the pregnant baboon takes a total of 30–45 minutes for the entire process due to challenges of the small size of the placenta in the first trimester.

Immunohistochemical quantification of uterine spiral artery remodeling:

SAR was quantified by immunohistochemical imaging in 15 untreated and 18 estradiol-treated baboons. A minimum of six randomly selected areas (5 mm^3) of placental basal plate were collected from each baboon for SAR analysis. Placental samples were fixed in 10% formalin, embedded in paraffin, sectioned (5 μm), and processed for hematoxylin/eosin histology and cytotrophoblast/epithelial cell-specific cytokeratin immunohistochemistry (12.5 mg/ml, 345779 CAM 5.2; BD Biosciences, San Jose, CA). Light microscopy (Nikon Eclipse E 1000 M; Tokyo, Japan) and an image analysis system (IP Lab version 3.63; Scanalytics, Inc., Fairfax, VA) were used to quantify the level of SAR in arteries of greater than 50 μm in diameter within the decidua basalis in each tissue sample as described previously[8,9]. Vessel diameter was assessed via a micrometer as the smallest distance across the center of the vessel lumen from the inside edge of the surrounding smooth muscle (not invaded) or cytotrophoblast (invaded) layers. The number of arteries exhibiting trophoblast invasion and remodeling was quantified by identifying spiral arteries in which the vessel wall was extensively (>50%) occupied by cytokeratin-positive cytotrophoblasts. The data are expressed as the percentage of SAR (i.e. number of trophoblast remodeled arteries divided by the total number of arteries counted). Although there were spiral arteries in which less than half of the vessel wall was occupied by trophoblasts, presumably reflecting partial adaptation, the numbers of the latter vessels were not quantified by immunohistochemical image analysis.

Statistical analysis:

Data were analyzed by the Student's *t* test for independent observations using GraphPad software (San Diego, CA). The baboon placenta consists of approximately 20 cotyledons[18,19] each supplied via a single spiral artery[20]. Each rendered B-flow/STIC M-mode image contained 1 to 3 different vessels and 4–10 spiral arteries were measured per animal or a total of 46 arteries in the untreated and 81 arteries in the estradiol-treated baboons were analyzed by B-flow/STIC imaging. The percentage of spiral arteries remodeled as quantified by immunohistochemical image analysis was obtained in a minimum of 12 spiral arteries per animal. The level of spiral artery luminal diameter as quantified by B-flow/STIC M-mode was correlated by linear regression with the level of percent SAR remodeling as quantified by immunohistochemical image analysis.

RESULTS

Serum estradiol levels and weights:

Mean (±SE) maternal saphenous vein serum estradiol levels on day 60 were approximately 4-fold greater ($P<0.01$) in estradiol-treated baboons than in untreated animals, while maternal mean arterial blood pressure and placental and fetal body weights were unaltered (Table 2).

Immunohistochemical quantification of SAR:

The median and first-third quartile values for the percentage of spiral arteries remodeled by extravillous trophoblasts, as quantified by immunohistochemical image analysis, was approximately 70% lower (P = 0.000001) in estradiol-treated baboons (11.52 [5.38 – 18.02]%) than in untreated animals (33.00 [28.60 – 46.80]%, Figure 2).

B-flow/STIC M-mode ultrasonography of spiral arteries:

As quantified by B-flow/STIC M-mode ultrasonography, the median and first-third quartile values for spiral artery luminal diameter at systole in SAR impaired baboons (1.1 [0.8 – 1.6] mm, Fig. 3A) was 32% lower (P = 0.014) than in untreated animals (1.6 [1.5 – 2.2] mm). Spiral artery luminal diameter was 50% lower (P = 0.005) at diastole in SAR suppressed baboons (0.5 [0.4 – 0.8] mm, Fig. 3B) than in untreated baboons (1.0 [0.8 – 1.1] mm). B-flow/STIC M-mode imaging and *ex vivo* quantification of the level of SAR were simultaneously performed in 9 of the untreated and estradiol-treated baboons. As shown in Fig. 4, the correlation coefficient between the level of spiral artery luminal diameter quantified at systole by B-flow/STIC M-mode and the percent of SAR quantified by immunohistochemical image analysis was $r = 0.67$, slope = 0.029 ($P < 0.05$).

Spiral artery volume flow was 85% lower (P = 0.014) in SAR suppressed baboons (0.33 [0.17 – 1.01] ml per cardiac cycle, Fig. 5) than in untreated animals (2.18 [1.00 – 2.75] ml per cardiac cycle).

DISCUSSION

The present study shows for the first time that B-flow/STIC M-mode ultrasonography provides a novel real-time noninvasive imaging method to detect a decrease in spiral artery luminal diameter reflecting movement of the vessel wall during the cardiac cycle in the first trimester in a nonhuman primate model of impaired SAR. Thus, spiral artery luminal diameter, as quantified by B-flow/STIC M-mode imaging, was 32% lower at systole and 50% lower at diastole in SAR suppressed baboons. The reduction in spiral artery luminal diameter was correlated with a decrease in the percent of spiral arteries remodeled by extravillous trophoblasts.

Although 3D power Doppler of the uteroplacental vascularization has identified pregnancies at risk for preeclampsia[21–25], prognostic value early in gestation is limited because power gain, pulse repetition frequency and other 3D settings compromise imaging. Other Doppler approaches, e.g. coherent flow power Doppler and superb microvascular imaging, have been employed to quantify placental vascularization and flow[26, 27], but clinical utility of Doppler is compromised by “blooming” artifacts, aliasing, signal drop out, and interference by fetal blood flow. In the present study, we employed B-flow/STIC M-mode ultrasonography, a non-Doppler technology that uses very short pulses with high spatio-temporal and contrast resolution to enable sharp rendering of vessel dimension. In the clinical setting, efficacy of a new imaging modality must be tested in a pilot case control study and subsequently in a large-scale population. We suggest that major strengths of the current study are the use of B-flow/STIC M-mode imaging and the nonhuman pregnant model, in which comparison of

real-time B-flow/STIC M-mode quantification of spiral artery luminal diameter was made with *ex vivo* quantification of the level of SAR by immunohistochemical image analysis in the first trimester of gestation, a time when such studies would be very difficult to undertake in human pregnancy.

We further suggest that the decrease in luminal diameter of the spiral arteries shown by B-flow/STIC M-mode imaging in the first trimester in SAR suppressed baboons reflects the impairment of remodeling into enlarged vessels with distensable walls and not a change in some other aspect of blood vessel development, e.g. an estrogen-induced increase in vessel proliferation into more numerous blood vessels of smaller diameter. Thus, the density of the uterine spiral arteries, i.e. total number of blood vessels per area of decidua basalis, was unaltered by estradiol administration early in baboon pregnancy[28].

Because the rate of blood flow through a vessel is proportional to the fourth power of vessel diameter[29], the 32–50% decrease in spiral artery diameter, as observed by B-flow/STIC M-mode in SAR suppressed baboons, would be expected to result in a marked reduction in blood flow and placental perfusion. Indeed, the present study shows that spiral artery volume flow was 85% lower in SAR suppressed than in normal baboons in the first trimester. In contrast, we previously showed that uterine artery volume flow, as quantified by Doppler ultrasound, was similar in value on day 60 of gestation in untreated (2.91 ± 0.38 ml/min/kg body weight) and estradiol-treated/SAR suppressed (2.90 ± 0.65) baboons, although Doppler was able to show an increase in downstream flow resistance near term in SAR suppressed animals[11]. Although an elevation in blood pressure can increase blood flow through the systemic vasculature, maternal arterial blood pressure was unaltered early in pregnancy in SAR suppressed baboons but became elevated by over 25% near term in SAR impaired baboons[11,13].

Along with the suppression of SAR, maternal vascular endothelial dysfunction was induced late in gestation in our baboon experimental model[13]. The latter pathophysiological manifestation is a hallmark of human preeclampsia[30–34]. Placental and fetal body weights of SAR impaired baboons were not altered in the first (Table 2) and third[11] trimesters of pregnancy despite the reduction in spiral artery volume flow and onset of maternal vascular dysfunction[13]. However, near term and after birth offspring derived from SAR impaired baboons appear to exhibit systemic vascular dysfunction (unpublished preliminary data), which has also been shown in offspring from human preeclampsia pregnancies[35]. Therefore, we propose that the current results obtained in a nonhuman primate translate to human pregnancy and indicate that B-flow/STIC M-mode ultrasonography provides a novel, safe and real-time imaging technology to quantify aspects of spiral artery dynamics that reflect the process of SAR. Future study will ascertain whether B-flow/STIC M-mode ultrasonography will uncover a deficiency in spiral artery luminal diameter reflective of SAR early in gestation in women who go on to exhibit the pathophysiological conditions associated with abnormal pregnancy such as preeclampsia.

We have recently reported[12] that noninvasive targeted delivery of the VEGF gene selectively to the maternal aspect of the placenta (but not the fetus) by contrast-enhanced ultrasonography/microsphere technology prevented the impairment of SAR as quantified by

immunohistochemical analysis in estradiol-treated baboons. The latter study showed that VEGF has a pivotal role in promoting spiral artery transformation during the first trimester of primate pregnancy. Future studies can be designed to ascertain whether detection of impairment of SAR by non-invasive B-flow/STIC M-mode ultrasound combined with targeted delivery of the VEGF gene early in pregnancy in estradiol-treated baboons provides an effective therapeutic intervention to prevent abnormal pregnancy. Positive results of such a study in the pregnant baboon would provide a basis for translational investigation of this treatment paradigm in adverse conditions of human pregnancy underpinned by improper SAR.

In conclusion, the present study shows that B-flow/STIC M-mode ultrasonography provides a novel real-time imaging method to detect a decrease in uterine spiral artery luminal diameter during the cardiac cycle early in pregnancy in a nonhuman primate model of impaired SAR.

ACKNOWLEDGEMENTS

The authors thank Irene Baranyk, B.A. for the computer-assisted preparation of this manuscript and Sandra Huband, B.A for the computer-assisted preparation of the graphs.

This study was supported by NIH R01 HD 93070 and R01 HD 93946 research grants.

REFERENCES

1. Brosens I A study of the spiral arteries of the decidua basalis in normotensive and hypertensive pregnancies. J Obstet Gynaecol Br Commonw 1964; 71: 222–230. [PubMed: 14138383]
2. Lyall F, Robson SC, Bulmer JN. Spiral artery remodeling and trophoblast invasion in preeclampsia and fetal growth restriction: relationship to clinical outcome. Hypertension 2013; 62: 1046–1054. [PubMed: 24060885]
3. Burton GJ, Fowden AL, Thornburg KL. Placental origins of chronic disease. Physiol Rev 2016; 96: 1509–1565. [PubMed: 27604528]
4. Llurba E, Turan O, Kasdaglis T, Harman CR, Baschat AA. Emergence of late-onset placental dysfunction: relationship to the change in uterine artery blood flow resistance between the first and third trimesters. Am J Perinatol 2013; 30: 505–512. [PubMed: 23254384]
5. Song WL, Zhao YH, Shi SJ, Liu XY, Zheng GY, Morosky C, Jiao Y, Wang XJ. First trimester Doppler velocimetry of the uterine artery ipsilateral to the placenta improves ability to predict early-onset preeclampsia. Medicine (Baltimore) 2019; 98: e15193. [PubMed: 31008942]
6. Taylor TJ, Quinton AE, deVries BS, Hyett JA. Uterine artery pulsatility index assessment at <11 weeks' gestation:a prospective study. Fetal Diagn Ther 2020; 47: 129–137. [PubMed: 31280268]
7. Benirschke K, Kaufmann P. Pathology of the Human Placenta. Springer-Verlag: New York, 2000; 220–223.
8. Bonagura TW, Pepe GJ, Enders AC, Albrecht ED. Suppression of extravillous trophoblast vascular endothelial growth factor expression and uterine spiral artery invasion by estrogen during early baboon pregnancy. Endocrinology 2008; 149: 5078–5087. [PubMed: 18566115]
9. Bonagura TW, Babischkin JS, Aberdeen GW, Pepe GJ Albrecht ED. Prematurely elevating estradiol in early baboon pregnancy suppresses uterine artery remodeling and expression of extravillous placental vascular endothelial growth factor and α1β1 and α5β1 integrins. Endocrinology 2012; 153: 2897–2906. [PubMed: 22495671]
10. Albrecht ED, Pepe GJ. Endocrinology of pregnancy. In Non-Human Primates in Perinatal Research, Brans YW, Kuehl TJ (eds). John Wiley & Sons: New York, 1988; 13–78.
11. Aberdeen GW, Bonagura TW, Harman CR, Pepe GJ, Albrecht ED. Suppression of trophoblast uterine spiral artery remodeling by estrogen during baboon pregnancy: impact on uterine and fetal

blood flow dynamics. Am J Physiol Heart Circ Physiol 2012; 302: H1936–H1944. [PubMed: 22427518]

12. Babischkin JS, Aberdeen GW, Lindner JR, Bonagura TW, Pepe GJ, Albrecht ED. Vascular endothelial growth factor delivery to placental basal plate promotes uterine artery remodeling in the primate. Endocrinology 2019; 160: 1492–1505. [PubMed: 31002314]
13. Albrecht ED, Babischkin JS, Aberdeen GW, Burch MG, Pepe GJ. Maternal systemic vascular dysfunction in a primate model of defective uterine spiral artery remodeling. American Journal of Physiology, Heart Circulatory Physiology 2021; 320: H1712–H1723. [PubMed: 33666502]
14. Turan S, Turan O, Baschet AA. Three- and four-dimensional fetal echocardiography. Fetal Diagn Ther 2009; 25: 361–372. [PubMed: 19786781]
15. Hongmei W, Ying Z, Ailu C, Wei S. Novel application of four-dimensional sonography with B-flow imaging and spatiotemporal image correlation in the assessment of fetal congenital heart defects. Echocardiography 2012; 29: 614–619. [PubMed: 22404098]
16. Dighe MK, Moshiri M, Jolley J, Thiel J, Hippe D. B-flow imaging of the placenta: a feasibility study. Ultrasound 2018; 26: 160–167. [PubMed: 30147740]
17. Urbaniak GC, Plous S. Research randomizer version 4.0 computer software. http://www.randomizer.org. [2013].
18. Houston ML, Hendrickx AG. Observations on the vasculature of the baboon placenta (Papio sp.) with special reference to the transverse communicating artery. Folia Primatol 1968; 9: 68–77.
19. Ramsey EM, Donner MW. Structure of the chorionic villi. In Placental Vasculature and Circulation, Ramsey EM, Donner MW (eds). W.B. Saunders Company: Philadelphia, 1980; p. 31.
20. Balasuriya H, Bell P, Waugh R, Thompson J, Gillin A, Hennessy A, Makris A. Primate maternal placental angiography. Placenta 2010; 31: 11–22. [PubMed: 19959226]
21. Dar P, Gebb J, Reimers L, Bernstein PS, Chazotte C, Merkatz IR. First-trimester 3-dimensional power Doppler of the uteroplacental circulation space: a potential screening method for preeclampsia. Am J Obstet Gynecol 2010; 203: 238.e1–e7. [PubMed: 20643389]
22. Rosner M, Dar P, Reimers LL. First-trimester 3D power Doppler of the uteroplacental circulation space and fetal growth restriction. Am J Obstet Gynecol 2014; 211: 521.e1–521.e8. [PubMed: 24834864]
23. Hashish N, Hassan A, El-Semary A, Gohar R, Youssef MA. Could 3D placental volume and perfusion indices measured at 11–14 weeks predict occurrence of preeclampsia in high-risk pregnant women? J Matern Fetal Neonatal Med 2015; 28: 1094–1098. [PubMed: 25007987]
24. Neto RM, Ramos JG. 3D power Doppler ultrasound in early diagnosis of preeclampsia. Pregnancy Hypertens 2016 ;6: 10–16. [PubMed: 26955765]
25. Eastwood KA, Patterson C, Hunter AJ, McCance DR, Young IS, Holmes VA. Evaluation of the predictive value of placental vascularization indices derived from 3-dimensional power Doppler whole placental volume scanning for prediction of pre-eclampsia: a systemic review and meta-analysis. Placenta 2017; 51: 89–97. [PubMed: 28089506]
26. Li YL, Dahl JJ. Coherent flow power Doppler (CFPD): flow detection using spatial coherence beamforming. IEEE Trans Ultrason Ferroelectr Freq Control 2015; 62: 1022–1035. [PubMed: 26067037]
27. Artul S, Nseir W, Armaly Z, Soudack M. Superb microvascular imaging: added value and novel applications. J Clin Imaging Sci 2017; 7: 45. [PubMed: 29404197]
28. Albrecht ED, Bonagura TW, Burleigh DW, Enders AC, Aberdeen GW, Pepe GJ. Suppression of extravillous trophoblast invasion of uterine spiral arteries by estrogen during early baboon pregnancy. Placenta 2006; 27: 483–490. [PubMed: 15990167]
29. Guyton AC, Hall JE. Guyton and Hall Textbook of Medical Physiology, Twelfth Edition. Saunders Elsevier: Philadelphia, 2011.
30. Roberts JM, Taylor RN, Musci TJ, Rodgers GM, Hubel CA, Mclaughlin MK. Preeclampsia: an endothelial cell disorder. Am J Obstet Gynecol 1989; 161(5): 1200–1204. [PubMed: 2589440]
31. Gilbert JS, Ryan MJ, LaMarca BB, Sedeek M, Murphy SR, Granger JP. Pathophysiology of hypertension during preeclampsia: linking placental ischemia with endothelial dysfunction. Am J Physiol Heart Circ Physiol 2008; 294: H541–550. [PubMed: 18055511]

32. Myatt L, Webster RP. Vascular biology of preeclampsia. J Thromb Haemost 2009;7 (3): 375–384. [PubMed: 19087223]

33. Ilekis JV, Tsilou E, Fisher S, Abrahams VM, Soares MJ, Cross JC, Zamudio S, Illsley NP, Myatt L, Colvis C, Costantine MM, Haas DM, Sadovsky Y, Weiner C, Rytting E, Bidwell G. Placental origins of adverse pregnancy outcomes: potential molecular targets: an executive workshop summary of the Eunice Kennedy Shriver National Institute of Child Health and Human Development. Am J Obstet Gynecol 2016; 215(1 Suppl): S1–S46. [PubMed: 26972897]

34. Rana S, Lemoine E, Granger JP, Karumanchi SA. Preeclampsia: pathophysiology, challenges, and perspectives. Circ Res 2019; 124(7): 1094–1112. [PubMed: 30920918]

35. Fox R, Kitt J, Leeson P, Aye CYL, Lewandowski AJ. Preeclampsia: risk factors, diagnosis, management, and the cardiovascular impact on the offspring. J Clin Med 2019; 8(10): 1625.

What are the novel findings of this work?

The present results show that B-flow/spatio-temporal image correlation (STIC) M-mode ultrasonography provides a novel, safe, real-time technology to quantify in the first trimester of baboon pregnancy a decrease in spiral artery luminal diameter, reflecting distensibility of the vessel wall, as an index of impaired spiral artery remodeling (SAR).

What are the clinical implications of this work?

This study is clinically significant since it shows that B-flow/STIC M-mode ultrasonography has the potential to be used as a screening tool to uncover and evaluate efficacy of new therapeutic modalities to prevent a defect in SAR early in gestation in women who go on to exhibit adverse pregnancy.

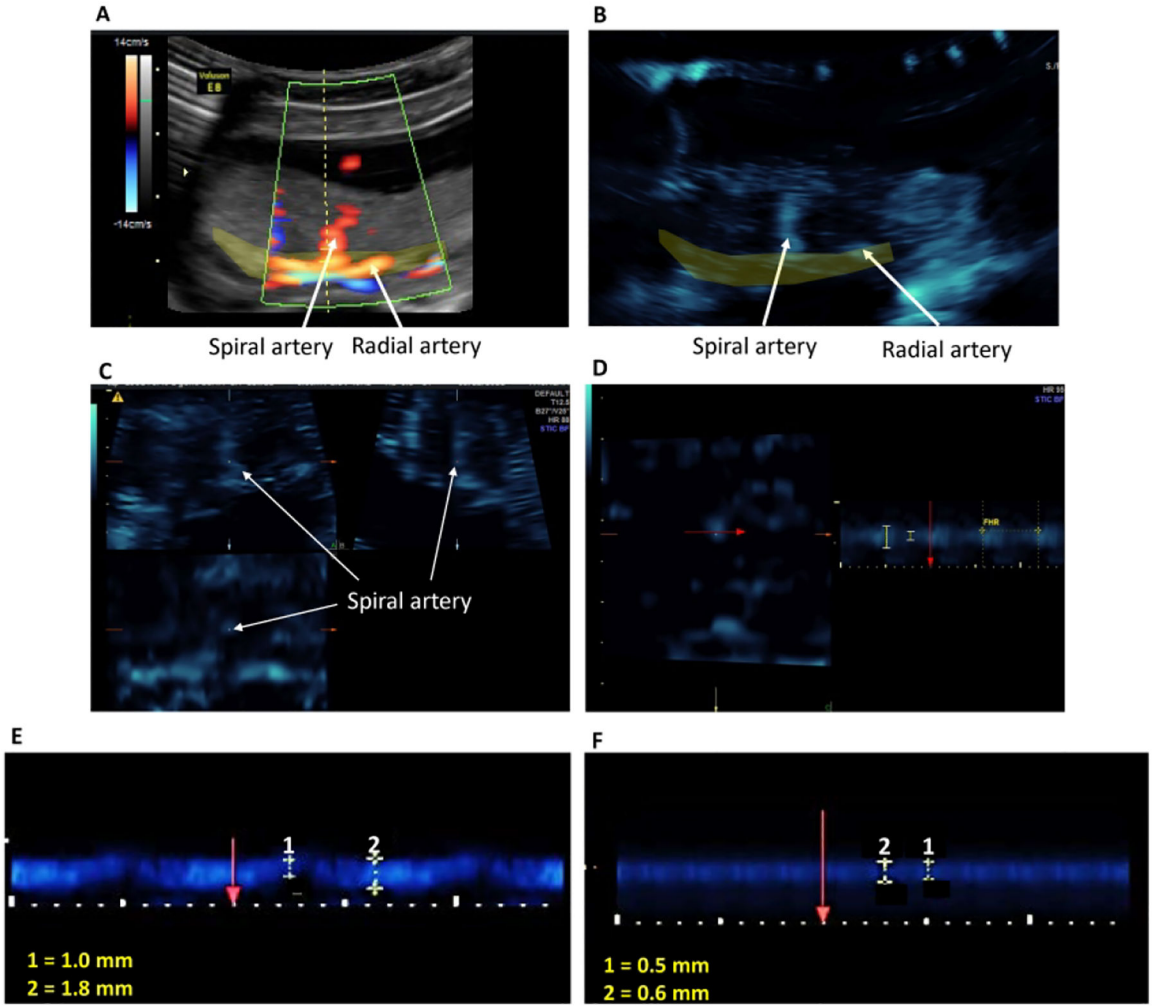

Figure 1:

Illustration of the B-Flow/STIC M-mode technique. A spiral artery was identified in the placental bed (yellow shaded area) using power Doppler (Panel A). B-flow was activated and the spiral artery was demonstrated at the same anatomical location (Panel B). A 4D- STIC block was acquired and the spiral artery was visible in 3 orthogonal planes (Panel C). M-mode was activated at the Z-axis and vessel luminal diameter was measured perpendicular (red arrow) to the vessel lumen (Panel D). Fetal heart rate (FHR) was measured each time to confirm that the blood vessel was a maternal vessel. Panels E and F show representative B-flow/STIC M-mode measurement of luminal diameters of two different spiral arteries during the cardiac cycle (1: diastole, 2: systole) in an untreated (E) and SAR suppressed (F) baboon.

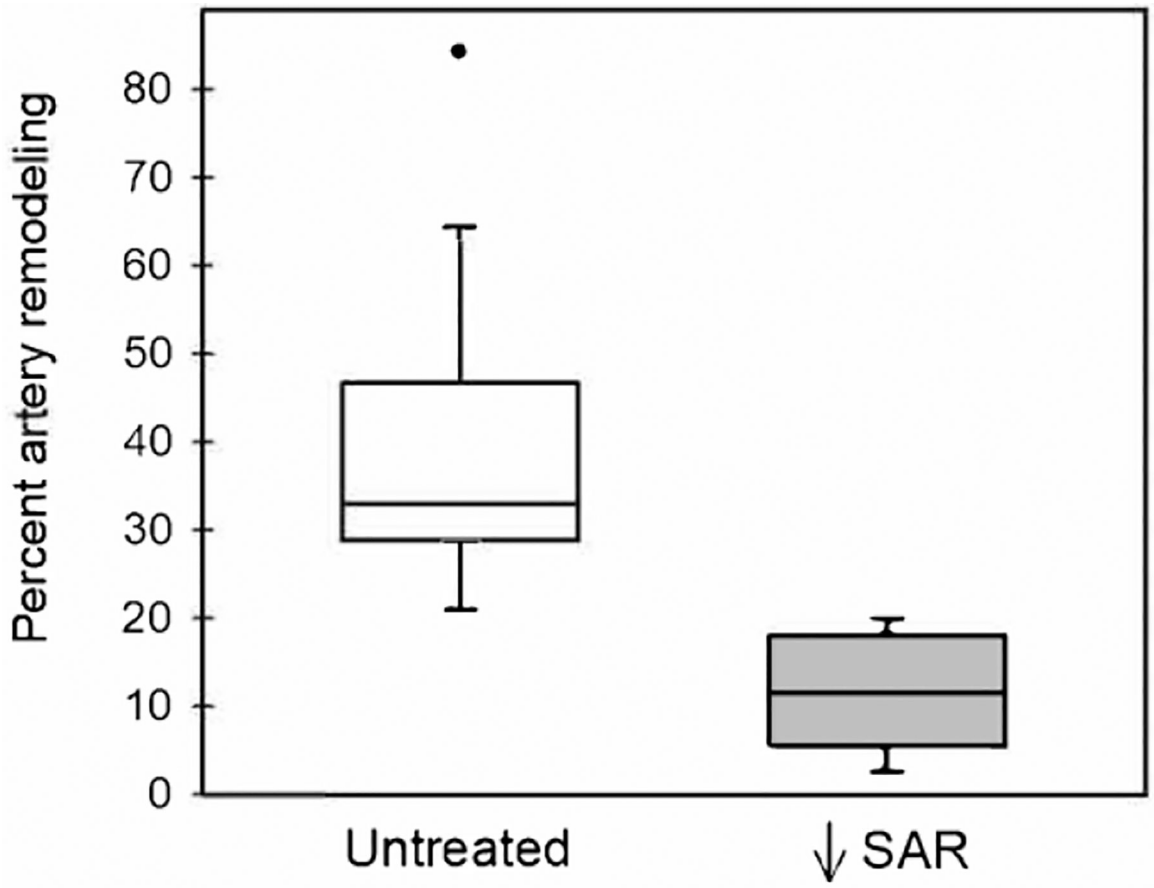

Figure 2:

Box-and-whisker plots showing the percentage of spiral artery remodeling (i.e. number of trophoblast invaded arteries divided by total number of arteries counted), as quantified by immunohistochemical image analysis, for vessels greater than 50 μm in diameter on day 60 of gestation in untreated (n = 15) and estradiol-treated (n = 18) baboons. Boxes are median (horizontal line) and interquartile range (IQR) and whiskers are the minimum and maximum range excluding one outlier (●) more than 1.5 × IQR.

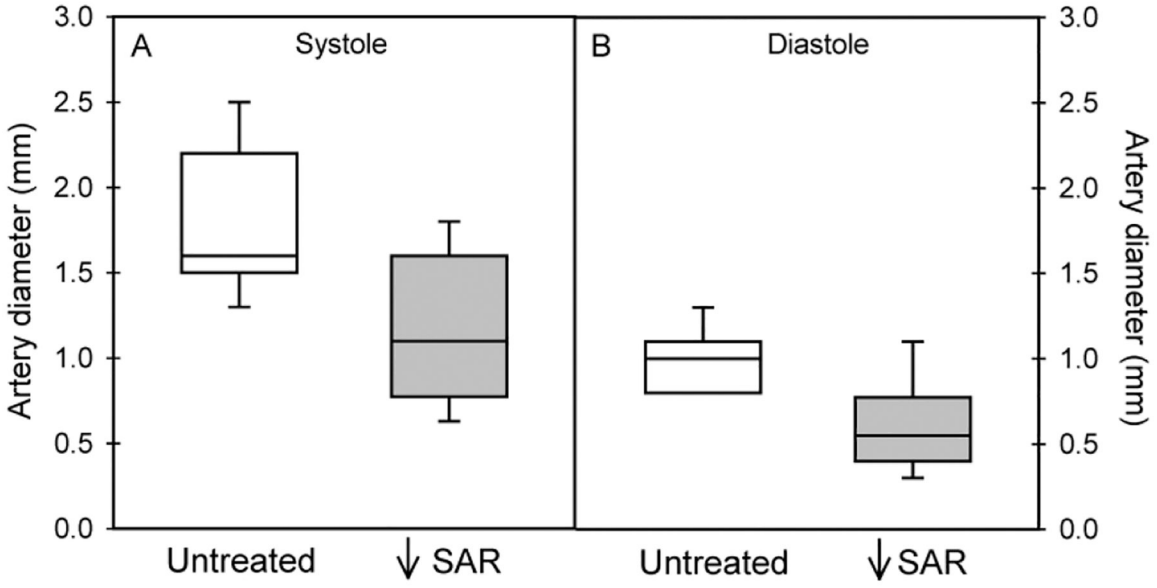

Figure 3:

Box-and-whisker plots showing spiral artery diameter at systole (panel A) and diastole (panel B) as quantified by B-flow/STIC M-mode ultrasonography on day 60 of gestation in untreated (n =7) and SAR suppressed (n = 12) baboons. The lowest value (0.8) is also the first quartile (i.e. no whisker) in untreated group (panel B).

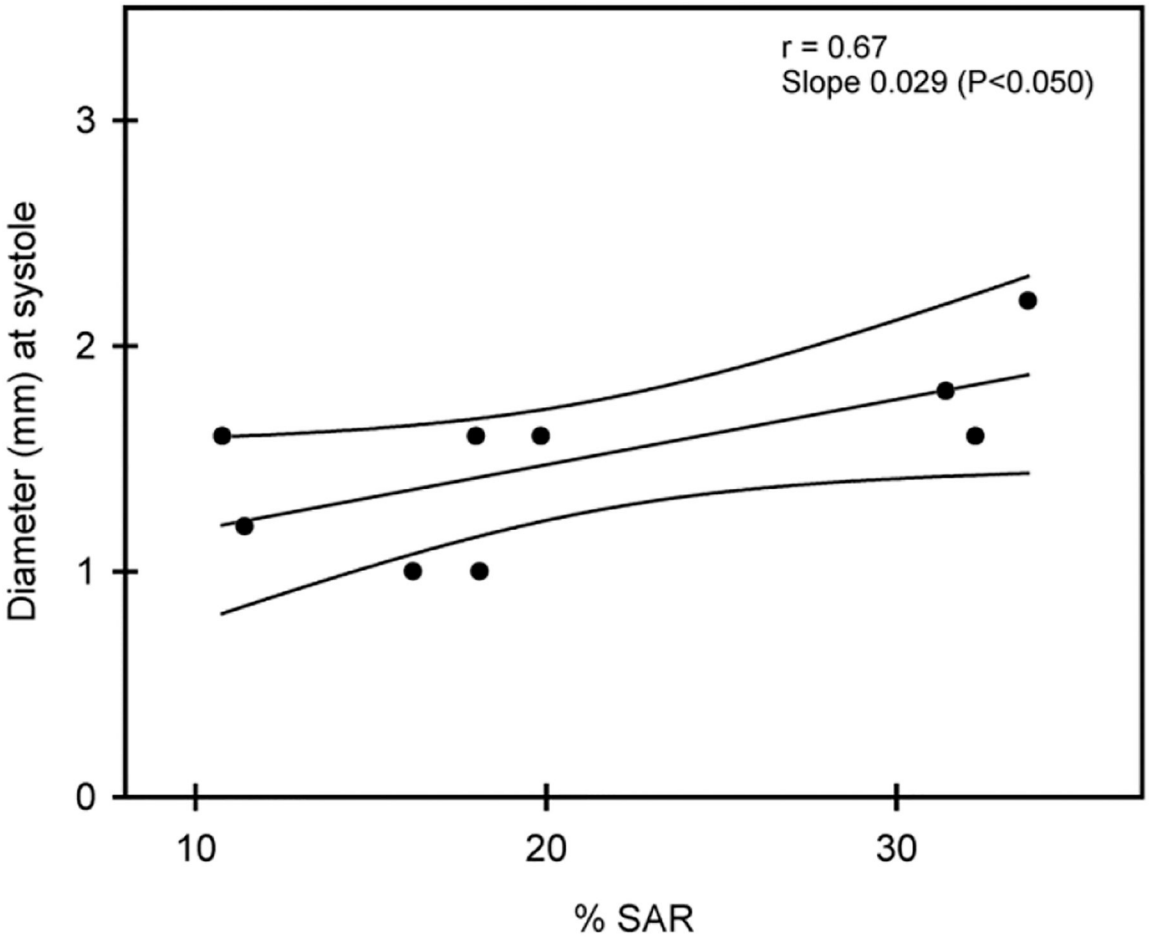

Figure 4:
Correlation coefficient and 95% confidence intervals of the level of spiral artery diameter as quantified by B-flow/STIC M-mode ultrasonography and percent of SAR as quantified by immunohistochemical image analysis on day 60 of gestation in 9 baboons.

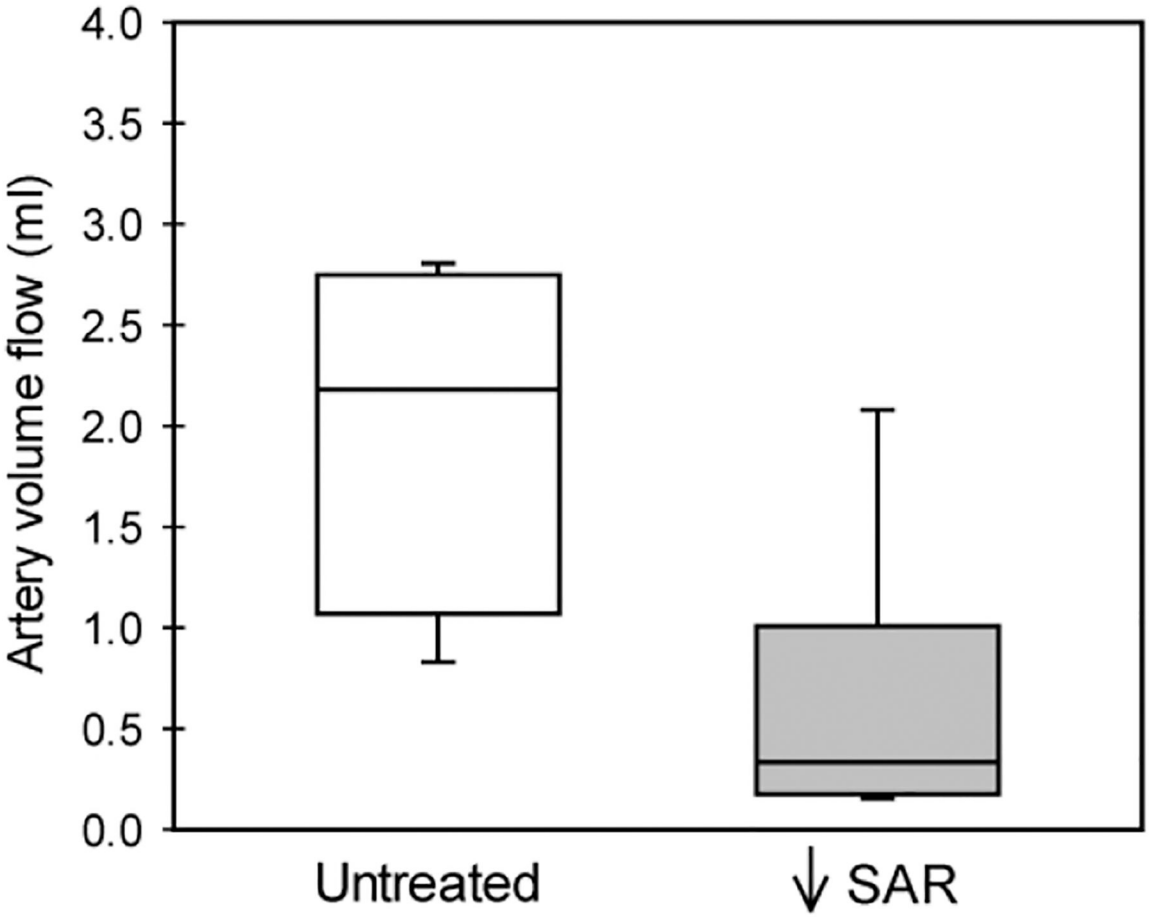

Figure 5:
Box-and-whisker plot showing spiral artery volume flow (ml per cardiac cycle) on day 60 in untreated (n = 4) and SAR suppressed (n = 8) baboons.

Table 1:

Nonhuman Primate Model of Defective SAR

Human preeclampsia	**Baboon model of defective SAR***
SAR ↓	SAR ↓
Uterine artery blood flow ↓	Uterine artery blood flow ↓
Maternal serum sFlt-1 levels ↑	Maternal serum sFlt-1 levels ↑
Maternal hypertension	Maternal hypertension
Maternal vascular endothelial dysfunction	Maternal vascular endothelial dysfunction

*Results from[8, 9, 11–13].

Table 2.

Maternal serum estradiol levels, blood pressure, and placental and fetal body weights in baboons

Treatment	N	Estradiol (ng/ml)	MABP (mm Hg)	Placental weight (g)	Fetal body weight (g)
Untreated	7	0.22 ± 0.02	71 ± 6	31.6 ± 0.3	12.1 ± 0.2
Estradiol	12	0.81 ± 0.06 *	72 ± 5	28.4 ± 0.5	11.5 ± 0.1

Means ± SE maternal saphenous vein serum estradiol levels, mean arterial blood pressure (MABP), and placental and fetal body weights on day 60 of gestation in baboons untreated or treated daily on days 25–59 of gestation (term = 184 days) with estradiol benzoate (25 μg/kg body weight/day, sc).

* Value different ($P < 0.01$) than in untreated baboons.